


RESEARCH ARTICLE

Open Access



Dependence receptor UNC5A restricts luminal to basal breast cancer plasticity and metastasis

Maria B. Padua^{1,8†}, Poornima Bhat-Nakshatri^{1†}, Manjushree Anjanappa¹, Mayuri S. Prasad¹, Yangyang Hao^{2,3}, Xi Rao^{2,3}, Sheng Liu^{2,3}, Jun Wan^{2,3}, Yunlong Liu^{2,3}, Kyle McElyea⁴, Max Jacobsen⁴, George Sandusky⁴, Sandra Althouse⁵, Susan Perkins⁵ and Harikrishna Nakshatri^{1,3,6,7*} 

Abstract

Background: The majority of estrogen receptor-positive (ERα⁺) breast cancers respond to endocrine therapies. However, resistance to endocrine therapies is common in 30% of cases, which may be due to altered ERα signaling and/or enhanced plasticity of cancer cells leading to breast cancer subtype conversion. The mechanisms leading to enhanced plasticity of ERα-positive cancer cells are unknown.

Methods: We used short hairpin (sh)RNA and/or the CRISPR/Cas9 system to knockdown the expression of the dependence receptor *UNC5A* in ERα⁺ MCF7 and T-47D cell lines. RNA-seq, quantitative reverse transcription polymerase chain reaction, chromatin immunoprecipitation, and Western blotting were used to measure the effect of *UNC5A* knockdown on basal and estradiol (E2)-regulated gene expression. Mammosphere assay, flow cytometry, and immunofluorescence were used to determine the role of *UNC5A* in restricting plasticity. Xenograft models were used to measure the effect of *UNC5A* knockdown on tumor growth and metastasis. Tissue microarray and immunohistochemistry were utilized to determine the prognostic value of *UNC5A* in breast cancer. Log-rank test, one-way, and two-way analysis of variance (ANOVA) were used for statistical analyses.

Results: Knockdown of the E2-inducible *UNC5A* resulted in altered basal gene expression affecting plasma membrane integrity and ERα signaling, as evident from ligand-independent activity of ERα, altered turnover of phosphorylated ERα, unique E2-dependent expression of genes effecting histone demethylase activity, enhanced upregulation of E2-inducible genes such as *BCL2*, and E2-independent tumorigenesis accompanied by multiorgan metastases. *UNC5A* depletion led to the appearance of a luminal/basal hybrid phenotype supported by elevated expression of basal/stem cell-enriched Δ Np63, CD44, CD49f, epidermal growth factor receptor (EGFR), and the lymphatic vessel permeability factor *NTN4*, but lower expression of luminal/alveolar differentiation-associated *ELF5* while maintaining functional ERα. In addition, *UNC5A*-depleted cells acquired bipotent luminal progenitor characteristics based on KRT14⁺/KRT19⁺ and CD49f⁺/EpCAM⁺ phenotype. Consistent with in vitro results, *UNC5A* expression negatively correlated with EGFR expression in breast tumors, and lower expression of *UNC5A*, particularly in ERα⁺/PR⁺/HER2⁻ tumors, was associated with poor outcome.

(Continued on next page)

* Correspondence: hnakshat@iupui.edu

[†]Equal contributors

¹Department of Surgery, Indiana University School of Medicine, Indianapolis, IN 46202, USA

³Center for Computational Biology and Bioinformatics, Indiana University School of Medicine, Indianapolis, IN 46202, USA

Full list of author information is available at the end of the article



(Continued from previous page)

Conclusion: These studies reveal an unexpected role of the axon guidance receptor *UNC5A* in fine-tuning ER α and EGFR signaling and the luminal progenitor status of hormone-sensitive breast cancers. Furthermore, *UNC5A* knockdown cells provide an ideal model system to investigate metastasis of ER α ⁺ breast cancers.

Keywords: Breast cancer, *UNC5A*, Netrin-1, Estrogen receptor, Estradiol and metastasis

Background

The luminal subtypes that express the estrogen receptor (ER) α represent approximately 70% of breast cancers, and the majority of these tumors respond to endocrine therapy [1]. However, resistance to endocrine therapy resulting in relapse is seen in approximately 30% of patients [1]. ER α ⁺ breast cancers are heterogeneous with at least two subtypes, luminal A and luminal B [2]. Luminal A tumors are estradiol (E2)-dependent and responsive to antiestrogens, whereas luminal B tumors display either intrinsic or acquired resistance to antiestrogens with an outcome almost similar to triple negative breast cancers (TNBCs) [3]. A subgroup of luminal A tumors, particularly those that have metastasized despite expressing luminal A biomarkers (ER α and progesterone receptor (PR)), do not respond to antiestrogen therapies and approximately 55% of these metastases have converted to a different subtype through an unknown mechanism [4].

Multiple mechanisms of antiestrogen resistance have been documented [5]. Most of the prior work focused on mechanisms that confer E2-independent activity to ER α , including kinases that phosphorylate ER α , co-activator molecules that enhance ER α activity, pioneer factors that govern chromatin binding of ER α , and growth factor receptor–ER α crosstalk [6–8]. However, to our knowledge, there have been limited attempts to decipher negative regulatory loops that may restrict ER α signaling subsequent to ligand-activated induction and deregulation of these negative regulatory loops leading to prolonged/sustained activation of ER α .

To identify luminal cell-expressed genes that may play a role in restricting E2-dependent proliferation, we scanned gene expression array datasets for E2-inducible genes with ER α binding sites and that have a growth inhibitory activity [9]. From this search, we focused on the dependence receptor (DR) pathways for their potential role in a negative feedback loop. Under physiological conditions, unliganded DRs elicit cell death and/or growth inhibition but elicit cell survival and proliferation when coupled with their ligands such as Netrin-1 (NTN1) [10]. DRs are direct transcriptional targets of p53 and integral to p53-dependent apoptotic pathways, particularly in the absence of ligands [11]. NTN1 belongs to the evolutionary conserved netrin family secreted proteins and is well characterized for its role in the nervous system [12]. Both netrins and DRs also play crucial roles in other systems, including development of the

mammary gland, inner ear, lungs, and pancreas [12, 13]. Loss of heterozygosity and homozygous deletion of DRs and upregulation of netrins are observed in a variety of cancers including breast cancer [11, 13]. These aberrations in DR–netrin pathways are believed to confer resistance to p53-dependent apoptosis and enhance proliferation of cancer cells.

In the present study, we show that *UNC5A* is an E2-inducible gene. Knockdown of *UNC5A* in ER α ⁺/PR⁺ cells resulted in defective turnover of phosphorylated ER α , enhanced E2 signaling, cell proliferation, and tumorigenesis independent of E2 supplementation accompanied with multiorgan metastases in xenograft models. Furthermore, *UNC5A* knockdown cells acquired a hybrid basal/luminal phenotype including elevated expression of epidermal growth factor receptor (EGFR). Thus, *UNC5A* could serve as a negative feedback molecule in ER α signaling, the deregulation of which could lead to breast cancer progression through enhanced plasticity.

Methods

Immunohistochemistry of tissue microarray (TMA)

Tissue samples were collected with Indiana University Institutional Review Board approval, informed patient consent, and HIPAA compliance. *UNC5A* and EGFR immunostaining was performed at the CLIA certified Indiana University Health Pathology Laboratory and scoring has been described previously [14]. *H* scores were calculated using stain intensity (0 to 3) multiplied by percent positive pixels (for *UNC5A*) or a formula based on stain intensity and number of weak, moderate, or strong positive pixels (for EGFR). For subjects with multiple tumor samples, only those with the highest *H* score were considered. Statistical analysis was performed on samples from 221 breast cancer patients, but only 196 patient samples (89%) had *UNC5A* values available. The log-rank test was used to compare patient and tumor variables between those with *UNC5A* *H* scores versus those without. The correlations between *UNC5A* and EGFR were determined by Spearman's correlation coefficient. For modeling the outcomes of overall survival and disease-free survival, the multivariate covariates used in the multivariate models from the individual reports for EGFR and *UNC5A* were included. Additionally, the *H* score information for EGFR and *UNC5A* were handled in three ways. First, the EGFR and *UNC5A* were dichotomized using the same optimal

cut-points as used in their individual reports. Secondly, the EGFR and *UNC5A* were dichotomized using their individual medians and cut-points. Finally, the continuous values were used in the models. Since EGFR was not linear, the natural log of EGFR was used in the models. For the models with continuous values, hazard ratios were calculated at the 25th, 50th, and 75th percentile of EGFR. Subgroup analyses were performed where the number of patients available was sufficient.

Cell lines

MCF7 and T-47D cells were obtained from American Tissue Culture Collection and cultured in minimum essential media (MEM) media as described previously [15]. TMCF7 cells correspond to cell lines derived from tumors developed in the mammary fat pad of nude mice implanted with MCF7 cells [16]. Cell lines were authenticated using Short Tandem Repeat Profiling Systems for cell line identification by a commercial vendor (DNA-center.com) in August 2012 and cell lines recreated from xenograft tumors were authenticated by Genetica (Burlington, NC, USA).

Short hairpin (sh)RNA and CRISPR constructs

The human *shRNA* lentiviral transduction particles for *sh5-UNC5A* and pLKO.1-puro vector control plasmids (*sh-Control*) were purchased from Sigma (cat. nos. SHCLNV-NM_133369 and SHC 001, respectively). The lentivector for *sh2-UNC5A* was obtained from Applied Biological Materials (cat. no. i026703g). CRISPR plasmids to target *UNC5A* were obtained from Sigma-Aldrich (HS0000509914).

Western blotting

Treatments consisted vehicle, heregulin- β 1 (HRG- β 1, R&D systems), E2, 4-hydroxy-tamoxifen (OHT), or ICI-182,780 (Sigma-Aldrich). The immunoblotting has been previously described [17] and details of antibodies are provided in Additional file 1. Although the majority of immunoblots were reprobbed with antibodies against ACTB (β -actin) as a loading control, only representative data per batch of cell lysates are shown.

RNA-seq and quantitative reverse transcription polymerase chain reaction (qRT-PCR)

cDNA was synthesized from 1 to 2 μ g of total RNA using the cDNA Synthesis Kit (Bio-Rad). qRT-PCR in duplicates from at least two biological replicates was performed with either Sybr-Green or TaqMan Universal PCR master mix and transcripts were analyzed in StepOnePlus and TaqMan 7900HT instruments (Applied Biosystems) with β -*ACTIN* as the normalization control. Fold-change was calculated by the $\Delta\Delta$ Ct method, whereas statistical analysis was performed on Δ Ct values. Primers

(Integrated DNA Technologies) and TaqMan probe details are shown in Additional file 1. RNA-seq of *sh-Control* and *sh5-UNC5A* cells treated for 3 h with vehicle or E2 was performed in triplicate as previously described [18], and raw sequencing data have been submitted to the gene expression omnibus (GEO; accession number GSE89700).

We used STAR RNA-Seq aligner to map all sequence libraries to the human genome (UCSC hg19) [19] followed by the assignment of uniquely mapped reads to individual genes based on annotation of hg19 refGene by featureCounts [20]. After trimmed mean of M values (TMM) normalization, gene expression profiling was summarized on the base-2 logarithmic scale. Genes with an average expression level lower than 1 for all phenotypes in MCF7 and T-47D cells, respectively, were excluded for further analysis. Differential expression (DE) analysis was performed using edgeR [21, 22] for special group comparisons in the study. All *p* values were corrected by multiple testing false discovery rate (FDR) adjustments. Genes with FDR < 0.05 and absolute value of fold change (FC) larger than 2 were determined as differentially expressed genes (DEGs).

Gene function enrichment analysis was performed using DAVID (<http://david.abcc.ncifcrf.gov/home.jsp> v6.8) [23, 24]. Significantly overrepresented gene ontology (GO) terms were selected if their *q* values (*p* values after FDR multiple test correction) were less than 0.05.

Promoter luciferase assay

Cells transfected with luciferase constructs were allowed to grow overnight in charcoal-dextran treated fetal calf serum (CCS) containing media followed by a 12-h E2 treatment. The Dual-Luciferase[®] Reporter assay (Promega) was performed according to the manufacturer's protocol.

Chromatin immunoprecipitation (ChIP) assay

ChIP assays for ER α binding on *UNC5A* and *BCL2* were performed under vehicle or E2 treatment for 45 min and 2 h as described previously [9].

Cell proliferation and mammosphere assays

After 24-h plating in regular media, the media was changed to CCS-containing media for 3 days and cells were treated with the indicated drug combinations. Cell proliferation was determined using the bromodeoxyuridine-incorporation enzyme-linked immunosorbent assay (ELISA) kit from Calbiochem after 5–6 days of plating with one media/drug change. Mammosphere assays with 5000 cells were performed as described previously [25].

Immunofluorescence

Cells grown on 35-mm glass-bottom culture dishes were fixed with 4% (w/v) paraformaldehyde for 10 min and permeabilized in phosphate-buffered saline (PBS) containing

0.15% (v/v) Triton X-100, 5% (v/v) donor goat serum (Gibco), and 1% (w/v) bovine serum albumin (Sigma-Aldrich) for 1 h. Cells were incubated with primary antibodies (Additional file 1) diluted in Dako antibody diluent (Dako; Agilent Technologies) for 90 min followed by 1-h incubation with the Alexa Fluor® 488 and 555 conjugated secondary antibodies (ThermoFisher Scientific). Nuclei was counterstained with Hoechst® 33,342.

Flow cytometry

Cells were stained with the indicated antibodies (Additional file 1) and analyzed in a LSR4 custom-made flow cytometer (BD Biosciences) as described previously [26].

Xenograft studies

The Indiana University Animal Care and Use Committee approved the use of animals in this study and all procedures were performed as per NIH guidelines. *sh-Control*, *sh2-UNC5A*, and *sh5-UNC5A* TMCF7 cells (2×10^6 in 100 μ l serum-free HBSS) were implanted into the mammary fat pad of 7-week-old female nude mice with or without a 60-day slow-release E2 pellet. Tumor growth was measured weekly and tumor volume was calculated as described previously [16]. After 12 weeks, the lungs and primary tumors were collected and processed for hematoxylin and eosin (H&E) and PECAM1 (CD31) staining. The whole slide digital imaging system of Aperio (ScanScope CS) was used for imaging of PECAM1-stained tumors. For the metastatic model, mice were inoculated with 2×10^5 TMCF7 cells into the left cardiac ventricle. Ovaries, spleen, and adrenal glands were collected within 17 weeks and processed as described above.

Statistical analysis

Statistical analyses were performed in GraphPad Prism® (6.02 version) or Statistical Analysis System (SAS; version 9.4) software with $p < 0.05$ considered as significant.

Results

UNC5A is a luminal cell-enriched gene and is E2 inducible

To determine E2-inducible signaling molecules that may dampen the E2 response or gene-specific E2 regulation and that are expressed at higher levels in luminal breast cancers compared with TNBCs, we first searched our previous microarray data of E2-regulated genes in MCF7 cells for known growth suppressive roles and then determined whether E2 directly regulated their expression by integrating E2-inducible gene expression with ER α ChIP-on-chip and ChIP-seq datasets. *UNC5A* suited these criteria as its expression was E2 inducible and ER α binding sites for this gene was detectable in ChIP-on-chip and ChIP-seq datasets [9, 27] (Fig. 1a). Furthermore, in 11 out of 12 studies in publicly available

Nuclear Receptor Signaling Atlas web resources showed 2- to 35-fold E2-inducible expression of *UNC5A* in MCF7 cells, uterus, and vagina (Additional file 2). We further confirmed E2-inducible expression of *UNC5A* in MCF7 cells by qRT-PCR (Fig. 1b) and Western blotting (see below), although induction at mRNA levels in our MCF7 cells was modest. Interestingly, the antiestrogen tamoxifen (OHT) failed to overcome the effect of E2 on *UNC5A* levels (Fig. 1b) suggesting unique effects of E2 on the expression of *UNC5A*. We used ChIP assay to verify ER α binding to one of the ER α binding sites (Fig. 1c). R2 Genomic and Visualization Platform (<http://r2.amc.nl>) analyses revealed a positive correlation between *UNC5A* and *ESR1* mRNA levels in breast cancer cell lines (Fig. 1d). Also, analyses of The Cancer Genome Atlas (TCGA) dataset for the relationship between *UNC5A* expression and breast cancer subtypes using the UALCAN program [28] revealed highest *UNC5A* expression in luminal breast cancers, which are usually ER α -positive, compared with TNBCs (Fig. 1e). In contrast, *NTN1* expression was higher in TNBCs compared with normal breast or luminal breast cancers (Fig. 1f).

Low *UNC5A* expression in primary breast cancers is associated with poor outcome

To obtain additional support for our hypothesis that a protein that attenuates ER α signaling has prognostic relevance, we performed immunohistochemical analyses of *UNC5A* in our previously described breast TMA in which 196 out of 221 tumors had measurable *UNC5A* expression [14] (Additional file 3). A representative staining pattern of *UNC5A* in breast tumor is shown in Fig. 2a. Tumor cells were moderate in staining in many of the cases with little to no background staining in the other tissues in the core (vascular endothelial cells, smooth muscle cells, fibroblasts, macrophages, and/or scattered lymphocytes infiltrating the tumor region). In both univariate and multivariate analyses, low *UNC5A* *H* score was associated with poor overall survival (Fig. 2b and Additional file 4). In subgroup analyses, in ER $^+$ /PR $^+$ /HER2 $^-$, lower *UNC5A* *H* score showed a trend of poor overall survival ($p = 0.055$) (Fig. 2c). *UNC5A* had no prognostic relevance when tumors were subgrouped broadly into ER $^+$ or ER $^-$ subgroups (Fig. 2d, e). Thus, *UNC5A* is a potential biomarker of outcome in a subgroup of breast cancer patients whose tumors express luminal A markers.

UNC5A knockdown results in enhanced ER α signaling

To model low *UNC5A* levels in cells with intact ER α -dependent signaling, we created *shRNA-UNC5A* MCF7 and T-47D cells, which express ER α and PR at different levels (Fig. 3a, b). MCF7 cells are more responsive to E2 than T-47D cells and, therefore, most of the experiments

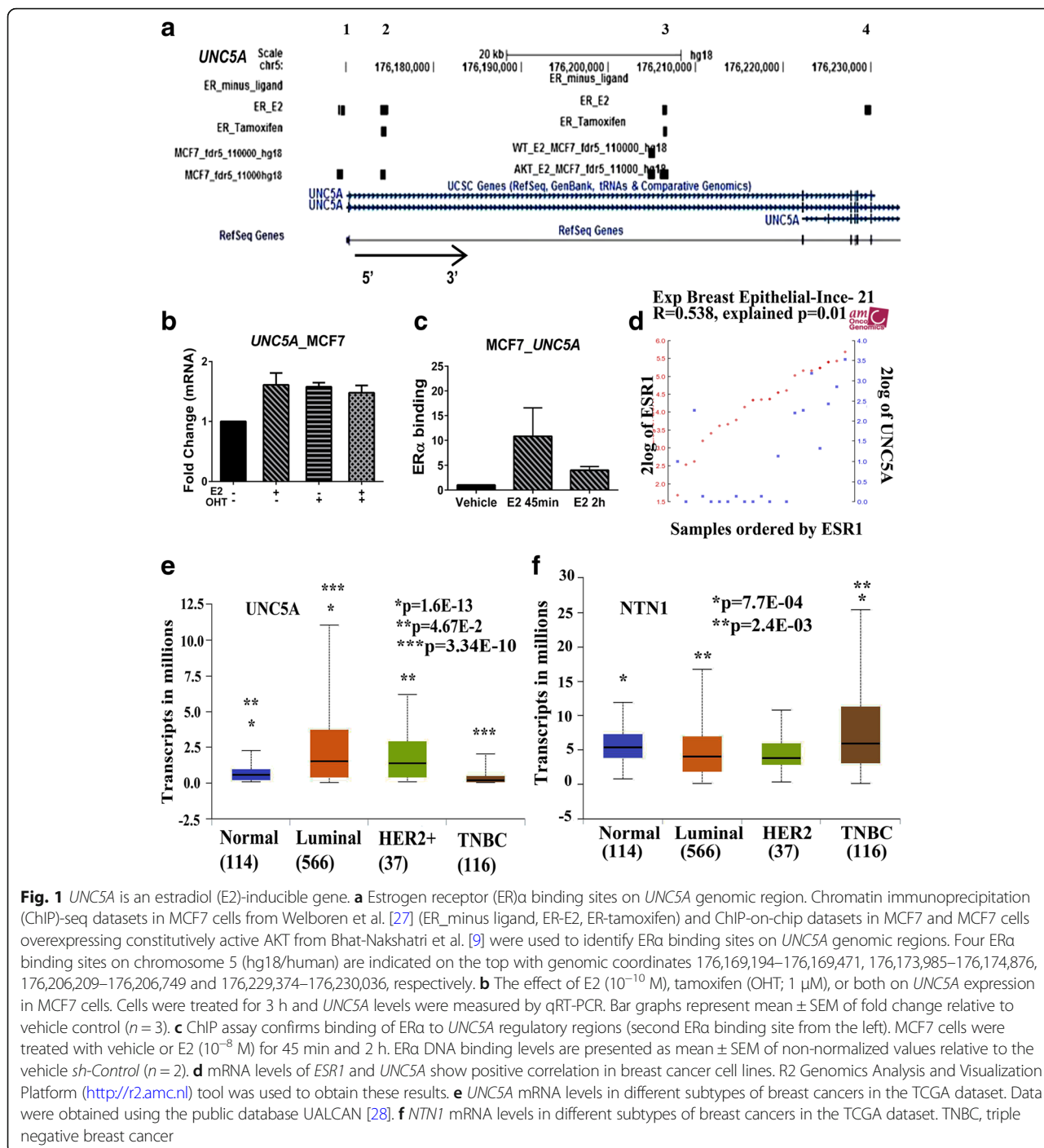


Fig. 1 *UNC5A* is an estradiol (E2)-inducible gene. **a** Estrogen receptor (ER) α binding sites on *UNC5A* genomic region. Chromatin immunoprecipitation (ChIP)-seq datasets in MCF7 cells from Welboren et al. [27] (ER_minus ligand, ER-E2, ER-tamoxifen) and ChIP-on-chip datasets in MCF7 and MCF7 cells overexpressing constitutively active AKT from Bhat-Nakshatri et al. [9] were used to identify ER α binding sites on *UNC5A* genomic regions. Four ER α binding sites on chromosome 5 (hg18/human) are indicated on the top with genomic coordinates 176,169,194–176,169,471, 176,173,985–176,174,876, 176,206,209–176,206,749 and 176,229,374–176,230,036, respectively. **b** The effect of E2 (10^{-10} M), or both on *UNC5A* expression in MCF7 cells. Cells were treated for 3 h and *UNC5A* levels were measured by qRT-PCR. Bar graphs represent mean \pm SEM of fold change relative to vehicle control ($n = 3$). **c** ChIP assay confirms binding of ER α to *UNC5A* regulatory regions (second ER α binding site from the left). MCF7 cells were treated with vehicle or E2 (10^{-8} M) for 45 min and 2 h. ER α DNA binding levels are presented as mean \pm SEM of non-normalized values relative to the vehicle *sh-Control* ($n = 2$). **d** mRNA levels of *ESR1* and *UNC5A* show positive correlation in breast cancer cell lines. R2 Genomics Analysis and Visualization Platform (<http://r2.amc.nl>) tool was used to obtain these results. **e** *UNC5A* mRNA levels in different subtypes of breast cancers in the TCGA dataset. Data were obtained using the public database UALCAN [28]. **f** *NTN1* mRNA levels in different subtypes of breast cancers in the TCGA dataset. TNBC, triple negative breast cancer

were performed in MCF7 cells with a few validation experiments in T-47D cells. *UNC5A* knockdown did not have an effect on ER α levels and the receptor underwent activation-coupled degradation upon E2 treatment in both *sh-Control* and *sh-UNC5A* cells (Fig. 3a, b). Note that E2 increased *UNC5A* protein in *sh-Control* but not in *sh-UNC5A* MCF7 cells (Fig. 3a). We note that this is the only commercially available antibody (Abcam, ab81165) that recognized protein of expected size but

showed variability in potency between batches. In transient transfection assay, estrogen response element (ERE)-driven luciferase-reporter gene showed elevated activity in vehicle-treated *sh-UNC5A* cells compared with *sh-Control* cells (Fig. 3c). In T-47D cells, which express higher levels of PR than MCF7 cells [29], *UNC5A* knockdown enhanced E2-inducible expression of *PGR* (Fig. 3d). In both MCF7 and T-47D cells, *UNC5A* knockdown substantially increased both basal (vehicle-treated) and, consequently,

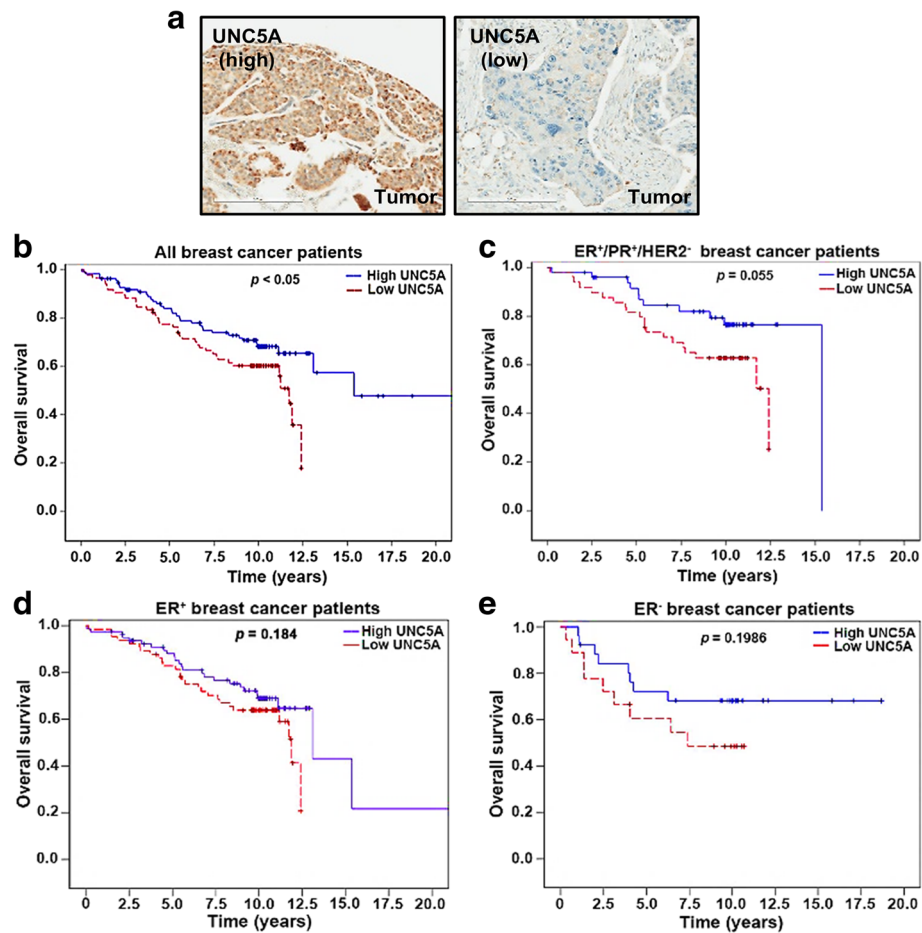


Fig. 2 Low UNC5A in breast tumors correlates with poor overall survival of breast cancer patients. **a** Representative UNC5A staining pattern in breast tumors with high or low expression (scale bars = 200 μ m). **b** Kaplan-Meier survival curves comparing overall survival of breast cancer patients with high (blue line) against low (red line) expression of UNC5A in tumors. Datasets were analyzed by log rank test from $n = 196$ patients. **c** Kaplan-Meier survival analysis of ER⁺/PR⁺/HER²- breast cancer patients according to the expression of UNC5A in tumors ($p = 0.055$) ($n = 98$). **d** Kaplan-Meier survival analysis of estrogen receptor (ER) α ⁺ breast cancer patients according to the expression of UNC5A in tumors ($n = 144$). **e** Kaplan-Meier survival analysis of ER α ⁻ breast cancer patients according to the expression of UNC5A in tumors ($n = 44$). PR, progesterone receptor

E2-inducible expression of BCL2 mRNA and protein (Fig. 3e, f). The enhanced BCL2 expression in *sh-UNC5A* cells correlated with increased E2-independent binding of ER α to the enhancer element of *BCL2* to which ER α and JMJD3 bind to create a poised chromatin [30] (Fig. 3g). To determine whether enhanced ER α activity in *UNC5A*-knockdown cells is due to altered phosphorylation of ER α , we used phospho-specific antibodies to determine the levels of ER α phosphorylated at S118 and S167. Phosphorylation of ER α at these residues is known to confer ligand-independent activity to the receptor [1]. Although we did not find any differences in basal phosphorylation status between *sh-Control* and *sh-UNC5A* cells, phosphorylated ER α underwent ligand-coupled degradation in *sh-Control* cells but not in *sh-UNC5A* cells (Fig. 3h). As a consequence, there was a modest difference in the rate of degradation of total ER α between clones.

These results suggest the need for signaling events downstream of *UNC5A* in turnover of phosphorylated ER α .

To determine whether the above observations of altered phospho-ER α turnover upon *UNC5A* knockdown show any relationship with cell proliferation, we measured cell proliferation under vehicle control and E2 \pm OHT-treated conditions. In MCF7 cells, *sh-UNC5A* increased proliferation under vehicle control, E2-, OHT-, and OHT plus E2-treated conditions compared with *sh-Control* to levels similar to E2-treated *sh-Control* cells (Fig. 3i, j). Although OHT reduced E2-inducible proliferation of *sh-UNC5A* cells, the overall proliferation rate of these cells under various treatments remained elevated compared with *sh-Control* cells. Collectively, these results suggest that *UNC5A* restricts the proliferation of ER α -positive cells.

To investigate whether enhanced the baseline proliferation of *sh-UNC5A* cells compared with *sh-Control* cells

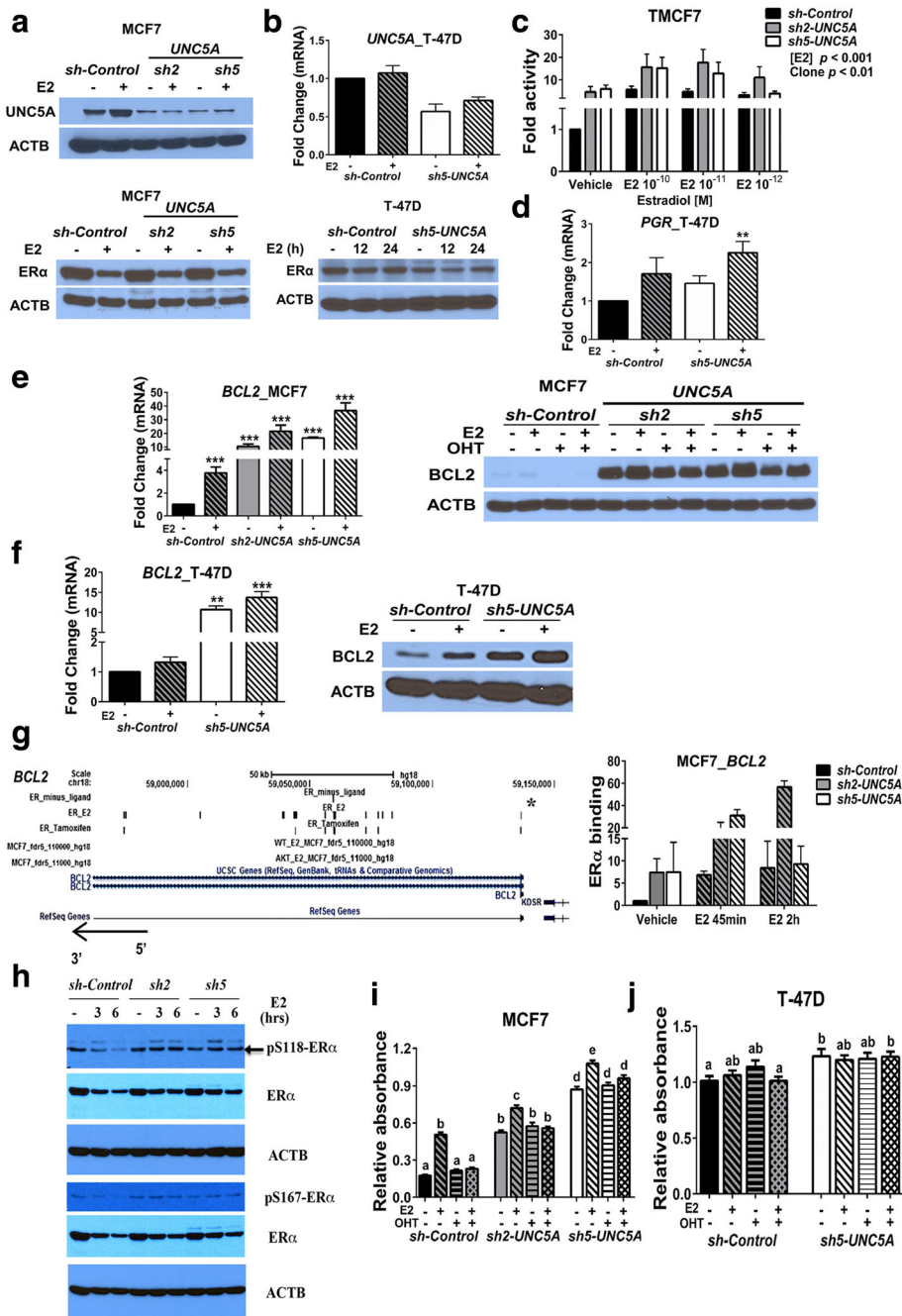


Fig. 3 (See legend on next page.)

(See figure on previous page.)

Fig. 3 Estradiol (E2)-regulated gene expression and response in cells on *UNC5A* knockdown. **a** *UNC5A* expression in *sh-Control* and *sh-UNC5A* transfected MCF7 cells (top). *sh2-RNA* and *sh5-RNA* target independent sequences of *UNC5A*. E2-inducible expression of *UNC5A* protein is evident in *sh-Control* but not in *sh-UNC5A* transfected MCF7 cells. Estrogen receptor (ER) α expression in *sh-Control* and *sh-UNC5A* MCF7 cells treated with or without E2 for 24 h (bottom). **b** Generation of T-47D cells expressing *sh-UNC5A* (top). shRNA expressing cells have lower *UNC5A* transcripts (mean \pm SEM; $n = 3$). As in MCF7 cells, *sh-UNC5A* had no effect on ER α protein levels in T-47D cells (bottom). **c** ERE-luciferase activity in *sh-Control* and *sh-UNC5A* MCF7 cells. Cells were treated with vehicle or three different concentrations of E2 for 12 h (mean \pm SEM; $n = 4$). Data were analyzed by two-way ANOVA where the main effects clone and [E2] were considered significant at $p < 0.01$ and $p < 0.001$, respectively. Note that ERE-luciferase activity was higher in *sh-UNC5A* clones in the absence of E2 treatment, although there was experimental variability. **d** *UNC5A* knockdown increases E2-inducible *PGR* expression in T-47D cells. Cells were treated with vehicle or E2 for 3 h ($n = 4$; $**p < 0.01$). **e** *UNC5A* knockdown leads to increased *BCL2* expression. *BCL2* mRNA (left) was measured in vehicle and E2-treated (3 h) *sh-Control* and *sh-UNC5A* MCF7 cells ($***p < 0.001$). *BCL2* protein levels were measured by Western blotting (right) in cells treated with vehicle, E2 (10^{-10} M), tamoxifen (OHT; 10^{-6} M), or an E2 and OHT combination for 24 h. **f** The effects of *UNC5A* knockdown on *BCL2* expression in T-47D cells. Cells were treated with vehicle control and E2 for 3 h (mRNA) or 24 h (protein) ($**p < 0.01$ and $***p < 0.001$). **g** *sh-UNC5A* enhances ER α binding to ERE-elements of *BCL2* in MCF7 cells. ER α binding sites on *BCL2* genomic regions identified using ChIP-seq and ChIP-on-chip data are shown in the left. ER α binding to ERE-elements (right most binding site indicated by a star in the ChIP-seq dataset, genomic coordinates, Chr18; 59,136,368–59,136,898) of *BCL2* was verified by ChIP-qPCR assay (mean \pm SEM of non-normalized values relative to vehicle *sh-Control*; $n = 2$). ER α binding in vehicle-treated *sh-Control* cells was set at 1 and the relative difference in other conditions is shown. **h** The effect of *UNC5A* knockdown on phosphorylated ER α . Cells were treated with E2 for 3 h or 6 h and the cell lysates were analyzed for ER α phosphorylated at S118 or S167 and total ER α . While phosphorylated ER α underwent activation-coupled degradation on E2 treatment in *sh-Control* cells, phosphorylated ER α was refractory to degradation in *sh-UNC5A* cells. **i** The effect of *UNC5A* knockdown on proliferation of *sh-Control* and *sh-UNC5A* MCF7 cells. Cells were treated for 5 days with vehicle control, E2, OHT, or E2 + OHT. Data are presented as mean of relative absorbance \pm SEM ($n = 2$, each with six technical replicates) and were analyzed by ANOVA. Bars with the same character/letters are not significantly different according to Tukey's test. For example, E2-induced proliferation rate of *sh-Control* cells is similar to the proliferation rate of vehicle-treated *sh-UNC5A* cells. **j** The effect of *UNC5A* knockdown on proliferation of T-47D cells. Assays were performed as in **i** and the statistical results are presented as in **i**

is ER α -dependent, we treated cells with ICI-182,780 (Fulvestrant) which degrades ER α . While ICI-182,780 reduced E2-induced proliferation of these cells, it had a minimal effect on baseline proliferation of all cell types (Additional file 5). These negative results can be interpreted in two ways: enhanced basal proliferation of *sh-UNC5A* cells compared with *sh-Control* cells is independent of ER α , or ER α in *sh-UNC5A* cells is less sensitive to ICI-182780-mediated degradation. Surprisingly, although ICI-182,780 caused degradation of total ER α in *sh-Control* and *sh-UNC5A* cells to a similar extent, ICI-182,780 increased the levels of ER α phosphorylated at S118 (Additional file 5). This unique effect of ICI-182,780 on phospho-ER α could explain the lack of its effects on the baseline proliferation rate of *sh-UNC5A* cells. Additional work is needed to clarify the role of ER α in the baseline proliferation rate of *sh-UNC5A* cells.

The dramatic effect of *UNC5A* on *BCL2* expression was puzzling. To ensure that this increase in *BCL2* expression is not due to aberrant integration of shRNAs into the genome, we used the CRISPR/Cas9 system to reduce *UNC5A* expression and selected single cell clones (Additional file 5). *UNC5A* protein levels were partially reduced in these single cell clones with an accompanying increase in *BCL2* expression. Thus, even a modest decrease in *UNC5A* protein levels was sufficient to trigger *BCL2* expression. We also observed stable *BCL2* overexpression in both *UNC5A* shRNA and CRISPR clones cultured for a prolonged time despite these clones regaining *UNC5A* protein expression as measured using the available antibody. Thus, it appears that

even transient knockdown of *UNC5A* leads to robust/permanent activation of *BCL2*, which is similar to previously reported stable activation of cancer germline genes upon transient knockdown of DNA methyltransferase 1 (DNMT1) [31].

Changes in gene expression associated with *UNC5A* knockdown

We performed RNA-seq of *sh-Control* and *sh5-UNC5A* MCF7 and T-47D cells treated with vehicle (basal) or E2 for 3 h and did pairwise comparisons to determine the effect of *UNC5A* on basal and E2-regulated gene expression (Fig. 4a). Genes were determined as DEGs for comparison if their FDR was < 0.05 and absolute value of fold change |FC| was > 2 (Fig. 4a and Additional file 6). Under basal growth conditions, *UNC5A* knockdown notably affected the expression of approximately 20% and 7% of genes in MCF7 and T-47D cells, respectively, potentially indicating its role in regulating the transcriptional machinery. For example, *APOBEC3B*, which is integral to ER α signaling [32], was one of the genes differentially expressed in *sh-UNC5A* cells compared with *sh-Control* MCF7 and T-47D cells (Additional file 6). We confirmed elevated expression of *APOBEC3B* in *sh-UNC5A* compared with *sh-Control* MCF7 cells (Fig. 4b). Based on the gene functional analysis using DAVID, genes differentially expressed in *UNC5A* knockdown MCF7 and T47-D cells were an integral part of the plasma membrane and extracellular region (Fig. 4c and Additional file 7). It is interesting to note that 167 DEGs in MCF7 cells were significantly overrepresented

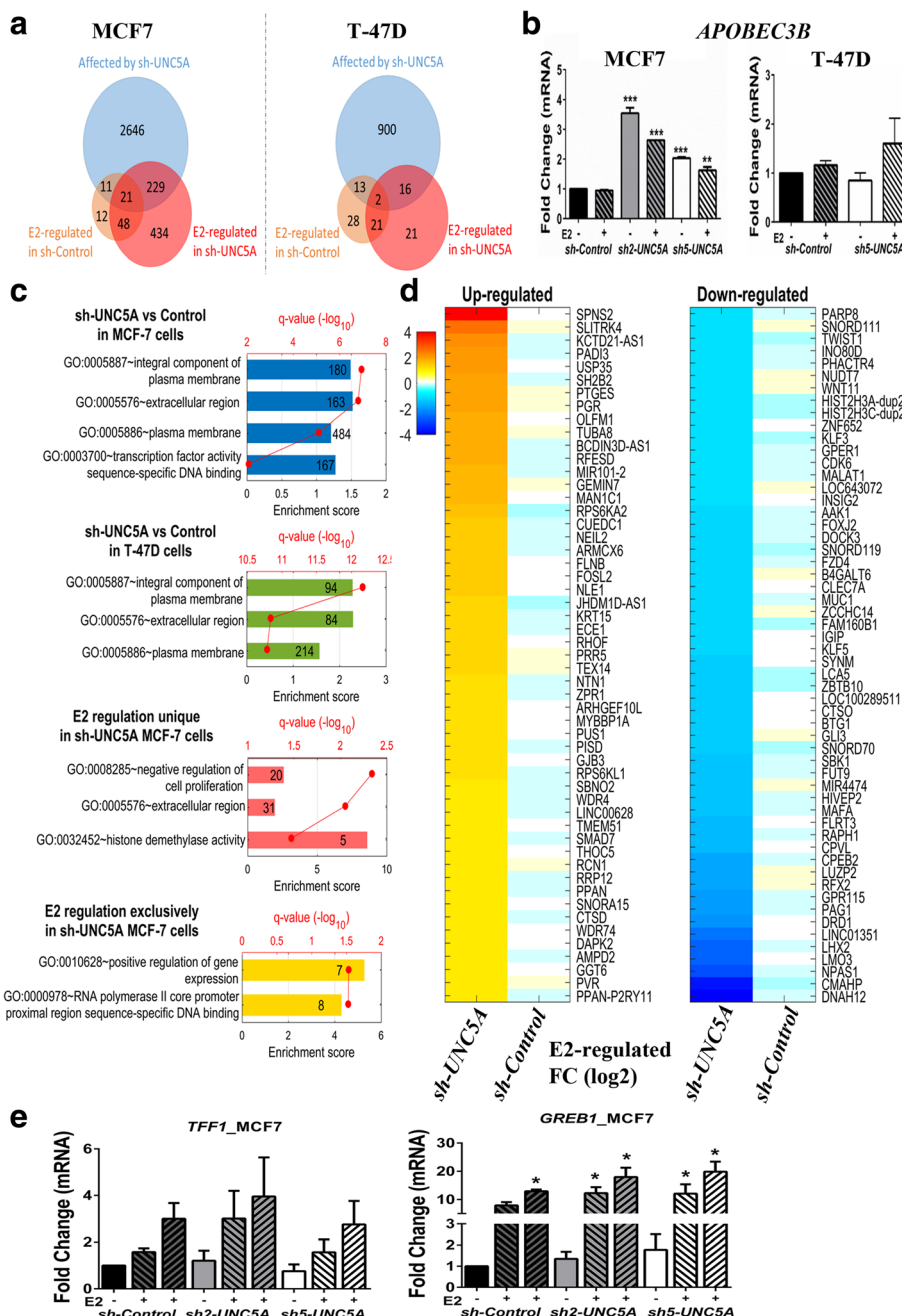


Fig. 4 The effect of UNC5A knockdown on basal and estradiol (E2)-regulated gene expression in MCF7 and T-47D cells. **a** Venn diagram showing the number of differentially expressed genes in *UNC5A* knockdown MCF7 and T-47D cells compared with *sh-Control* cells with and without 3 h E2 treatment. **b** *UNC5A* knockdown MCF7 but not T-47D cells express higher levels of *APOBEC3B* (** $p < 0.01$ and *** $p < 0.001$). **c** Signaling pathways affected by *UNC5A* knockdown under vehicle and E2-treated conditions. The number of genes in each of the networks is shown and name of the genes in each network and fold changes in expression are presented in Additional files 7 and 6, respectively. *UNC5A* affected mainly basal gene expression in T-47D cells. The gene set 'E2 regulation unique in *sh-UNC5A* MCF7 cells' corresponds to those genes whose magnitude of E2-regulated expression differed from *sh-Control* cells, although these genes may be E2-regulated in both cell types. The gene set 'E2 regulation exclusively in *sh-UNC5A* MCF7 cells' corresponds to those genes whose expression was E2-regulated only in *sh-UNC5A* cells. **d** Heatmap of genes uniquely upregulated or downregulated by E2 in *sh-UNC5A* MCF7 cells. E2 did not affect their expression in *sh-Control* MCF-7 cells. **e** The effect of *UNC5A* knockdown on basal and E2-inducible expression of TFF1 and GREB1. TFF1 and GREB1 expression was measured by qRT-PCR in vehicle, 3-h, and 6-h E2-treated cells. GREB1 expression in 3-h and 6-h E2 treated *sh-UNC5A* cells was modestly but significantly higher compared with E2-treated *sh-Control* cells (indicated by *)

in sequence-specific transcription factor DNA binding activity (Fig. 4c). *UNC5A* knockdown also had a significant effect on E2-regulated gene expression, particularly in MCF7 cells. A total of 434 genes were recognized as undergoing significant changes in gene expression by E2 in *sh-UNC5A* MCF7 cells, whereas only 21 genes were identified as DEGs in *sh-UNC5A* T-47D cells (Fig. 4a and Additional file 6). In *sh-UNC5A* MCF7 cells but not in *sh-Control* cells, E2-targeted genes were associated with negative regulation of cell proliferation, extracellular region, and histone demethylase activity (Fig. 4c). For example, E2 induced the expression of histone demethylases KDM4B and KDM7A but reduced the levels of UTY and ARID5B in *sh-UNC5A* but not in *sh-Control* MCF7 cells [33] (Additional file 6). JARID2, which regulates the polycomb complex and histone methyltransferases [34], was E2 inducible in *sh-UNC5A* but not in *sh-Control* MCF7 cells (Additional file 6). Furthermore, we found that 109 out of these 434 genes (Fig. 4d) were not regulated by E2 in *sh-Control* MCF7 cells ($FDR > 0.5$ and $|FC| < 1.15$), whereas their expression was under E2 control in *sh-UNC5A* MCF7 cells. These 109 genes are associated with positive regulation of gene expression and affect transcriptional regulation by RNA polymerase II (Fig. 4c). By contrast, no specific GO functions could be assigned to uniquely E2-regulated genes in *sh-UNC5A* T-47D cells. We note that the effect of *UNC5A* on E2-regulated genes is gene-specific since *sh-Control* and *sh-UNC5A* MCF7 cells showed similar levels of E2-regulated expression of TFF1 and only a modest effect on E2-regulated expression of GREB1, two commonly used genes to measure E2-inducible genes (Fig. 4e). Collectively, these results indicate a cell type-dependent role of *UNC5A* in controlling basal and E2-regulated gene expression with potential downstream effects ranging from plasma membrane composition to transcriptional output from RNA polymerase II.

***UNC5A* knockdown results in nonclassical luminal/basal hybrid gene expression pattern**

UNC5A knockdown increased the levels of oncogenic $\Delta Np63$ isoform mRNA while simultaneously lowering the expression of tumor suppressive *TAp63* isoform [35] (Fig. 5a, b). *TP63* is an E2-repressed gene and ER α failed to repress $\Delta Np63$ in *sh-UNC5A* clones with efficient *UNC5A* knockdown (*sh5-UNC5A* clones of MCF7 and T-47D; Fig. 5a, b). Overall, $\Delta Np63$ levels \pm E2 treatment remained elevated in *sh-UNC5A* cells compared with *sh-Control* cells. RNA-seq studies showed lower expression of luminal/alveolar differentiation-associated *ELF5* but elevated expression of the pro-oncogenic *MECOM* (*EVI-1*) and lymphangiogenic *NTN4* [36–38] in *sh-UNC5A* cells compared with *sh-Control* cells (Additional file 6). Indeed, *ELF5* levels were significantly lower and *NTN4*

levels were higher in *sh-UNC5A* cells compared with *sh-Control* cells (Fig. 5c, d). *MECOM* protein was undetectable in MCF7 cells but elevated in *sh-UNC5A* T-47D cells compared with *sh-Control* cells (Fig. 5e). In addition, while *sh-Control* cells expressed mainly KRT19, *sh-UNC5A* cells expressed either KRT14, KRT19, or both KRT14 and KRT19 (basal and luminal cytokeratins, respectively) [39] (Fig. 5f and Additional file 8). Bipotent luminal progenitor cells are KRT14 and KRT19 double-positive [40]. Note that *UNC5A* knockdown did not result in the morphologic features of epithelial to mesenchymal transition (EMT), nor did it result in the expression of EMT-associated genes such as *SNAI1*, *SNAI2*, *ZEB1*, or *ZEB2* (Additional file 6 and data not shown). However, we observed elevated expression of *ITGB6* (Integrin $\beta 6$) in *sh-UNC5A* cells compared with *sh-Control* cells (Additional file 6); *ITGB6* is pro-oncogenic and is induced during EMT of colon cancer cells [41].

Since $\Delta Np63$ maintains stem cell phenotype and cancer cells with hybrid luminal/basal/mesenchymal characteristics display enhanced cancer stem cell (CSC) properties [35, 42], we used mammosphere assays and flow cytometry to characterize *sh-Control* and *sh-UNC5A* MCF7 cells for stemness. While mammospheres of *sh-Control* were well organized, *sh-UNC5A* cells formed irregular mammospheres (Fig. 5g). In addition, while *sh-Control* cells were predominantly CD49f (ITGA6)⁻/EPCAM⁺, a subpopulation of *sh-UNC5A* cells showed CD49f⁺/EPCAM⁺ phenotype (Fig. 5h). CD49f⁺/EPCAM⁻, CD49f⁺/EPCAM⁺, and CD49f⁻/EPCAM⁺ cells display stem/basal, luminal progenitor, and differentiated/mature features, respectively [43]. *Sh-Control* cells showed CD44⁻/CD24⁺ non-CSC phenotype whereas *sh-UNC5A* cells acquired the features of CSCs as evident from the presence of CD44⁺/CD24⁺ and CD44⁺/CD24⁻ cells [44]. Furthermore, *sh-UNC5A* MCF7 cells expressed significantly higher levels of stemness-associated *SOX2* [45] (Additional file 6).

***UNC5A* knockdown results in elevated EGFR expression and AKT activity**

Two of our observations and one prior report prompted us to investigate whether *UNC5A* knockdown is associated with altered activity of EGFR, which could explain the effects of *UNC5A* on E2-regulated gene expression. First, we observed enhanced basal ERE-luciferase activity in *sh-UNC5A* cells, suggesting ligand-independent activity of ER α which typically involves growth factor receptor–ER α crosstalk [46]. EGFR is forefront in this crosstalk as it can alter ER α cistrome and ER α -regulated gene expression [47]. Second, *sh-UNC5A* cells showed luminal/basal hybrid phenotype, and EGFR activation is common in cells with basal phenotype [48]. Third, a recent study showed that *NTN1*, in the absence of

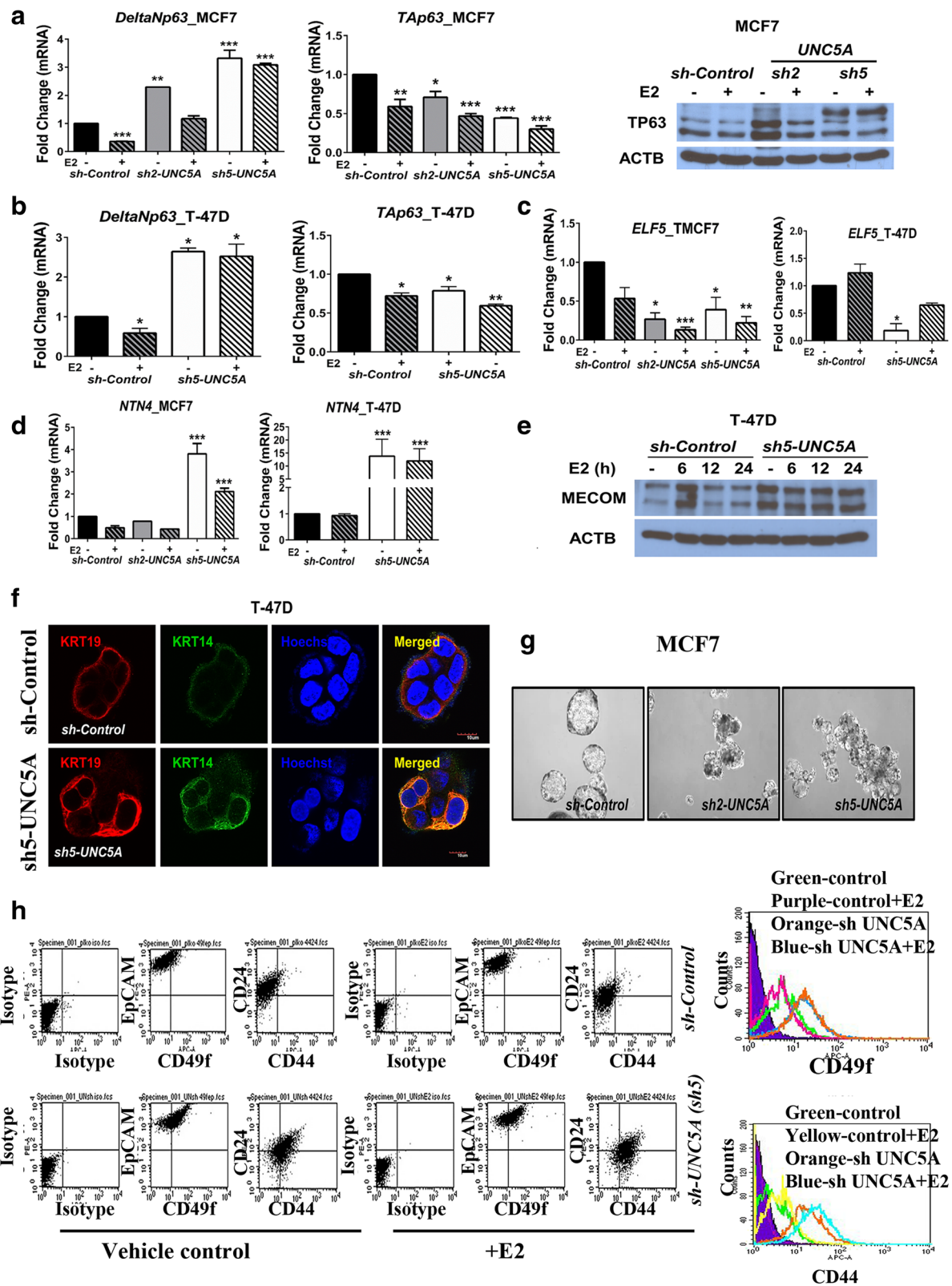


Fig. 5 (See legend on next page.)

(See figure on previous page.)

Fig. 5 *UNC5A* knockdown results in luminal/basal hybrid and bipotent luminal progenitor phenotype. **a** $\Delta Np63$ levels are significantly elevated in *sh-UNC5A* MCF7 cells. Cells were treated with vehicle or estradiol (E2) for 3 h and qRT-PCR was used to measure $\Delta Np63$ and *Tap63* levels (mean \pm SEM, $n = 2$). Data were analyzed as in Fig. 3e (* $p < 0.05$, ** $p < 0.01$, and *** $p < 0.001$). TP63 protein levels in *sh-Control* and *sh-UNC5A* MCF7 cells treated with or without E2 for 24 h are shown on the right. TP63 is expressed as multiple isoforms and there appears to be isoform switching in *sh-UNC5A* cells compared with *sh-Control* cells. **b** $\Delta Np63$ and *Tap63* levels in *sh-Control* and *sh-UNC5A* T-47D cells. **c** *sh-UNC5A* cells have lower *ELF5* mRNA compared with *sh-Control* cells. Cells were treated with vehicle or E2 for 3 h and qRT-PCR was used to measure *ELF5*. **d** *UNC5A* knockdown leads to elevated *NTN4*. **e** *UNC5A* knockdown leads to elevated *MECOM* (EVI-1) expression in T-47D cells. Although *MECOM* levels were elevated in MCF7 cells upon *UNC5A* knockdown (Additional file 6), proteins were not detected by Western blotting. **f** *UNC5A* knockdown T-47D cells express both KRT14 (basal; green) and KRT19 (luminal; red) while *sh-Control* T-47D cells express luminal KRT19. Results for TMCF7 cells are shown in Additional file 8. **g** *sh-UNC5A* MCF7 cells form irregularly shaped mammospheres. **h** *UNC5A* knockdown MCF7 cells display phenotypic characteristics similar to luminal progenitor (CD49f⁺/EPCAM⁺)/cancer stem cells (CD44⁺/CD24⁻) compared with *sh-Control* cells. A histogram displaying CD49f and CD44 expression in different cell types is depicted on the right

UNC5A, increases EGFR at the post-translational level [49]. We first measured EGFR levels in *sh-Control* and *UNC5A* knockdown cells. EGFR protein but not mRNA levels were significantly higher in *sh-UNC5A* cells compared with *sh-Control* cells (Fig. 6a and data not shown). AKT and ERK are the two major kinases activated downstream of EGFR that can increase ligand-independent activity of ER α [1]. We determined whether *UNC5A* knockdown had an effect on vehicle, E2-regulated, and HRG β 1-induced activation of these kinases. *sh-UNC5A* cells showed robust activation of AKT as measured by pAKT-S473 levels but not ERK (Fig. 6b). We recently reported that AKT1 but not AKT2 is active in MCF7 cells [17]. Immunoblotting using isoform-specific phospho-antibodies showed upregulation of pAKT1 but not pAKT2 in *sh-UNC5A* cells compared with *sh-Control* cells (Fig. 6c). These results indicate a negative relationship between EGFR and *UNC5A* expression in cell line models. Similarly, *UNC5A* and EGFR expression showed negative correlation in breast tumor samples when the analyses included all samples or only ER⁺ samples (Fig. 6d).

We next investigated the role of ER α in negative crosstalk between *UNC5A* and EGFR/TP63. Treatment of cells with ICI-182,780 results in degradation of ER α and, consequently, elevated expression of genes typically repressed by ER α . Indeed, treatment of *sh-Control* MCF7 and T-47D cells caused degradation of ER α with a concomitant increase in TP63 (Fig. 6e). Interestingly, ICI-182,780 treatment did not have an effect on EGFR but reduced the level of TP63 in *sh-UNC5A* cells (Fig. 6e). Similar to TP63, elevated expression of BCL2 upon *UNC5A* knockdown is ER α -dependent as its levels were lower in ICI-182,780-treated cells compared with untreated *sh-UNC5A* cells (Fig. 6e). Thus, while elevated EGFR levels in *sh-UNC5A* cells are ER α -independent, $\Delta Np63$ and BCL2 upregulation in these cells is at least partially ER α -dependent.

***sh-UNC5A* cells form metastatic tumors independent of E2 supplementation**

MCF7 cells form nonmetastatic tumors in female nude mice when injected with matrigel or when supplemented

with E2 pellets, although there is less uniformity between the sizes of tumors between animals [16]. We had previously reported in the MDA-MB-231 model that cell lines derived from tumors that develop in the mammary fat pad upon implantation of parental cells show enhanced and uniform tumorigenicity upon re-implantation [50]. We used this approach to increase uniformity in tumorigenicity and generated TMCF7 *sh-Control*, *sh2-UNC5A*, and *sh5-UNC5A* cells. As with MCF7 cells, *sh-UNC5A* TMCF7 cells showed elevated BCL2 and $\Delta Np63$ compared with *sh-Control* cells (Additional file 8). *sh-UNC5A* but not *sh-Control* TMCF7 cells displayed KRT14/KRT19 double-positive phenotype (Additional file 8). A large subpopulation of *sh-UNC5A* TMCF7 cells was of the CD44⁺/CD24⁺ and CD49f⁺/EPCAM⁺ phenotype compared with *sh-Control* cells (Additional file 8), and mammospheres formed by these cells were irregular compared to mammospheres from *sh-Control* cells (Additional file 8). In addition, *sh-UNC5A* TMCF7 cells expressed significantly higher levels of SOX2 despite maintaining ER α expression (Additional file 8). Consistent with RNA-seq data (Additional file 6), a large subpopulation of *sh-UNC5A* TMCF7 cells were ITGB6⁺ compared with *sh-Control* cells (Additional file 8).

A significant number of mice injected with *sh-UNC5A* cells but not *sh-Control* cells developed tumors in the absence of E2 pellets (Fig. 7a). The size of these tumors was larger than tumors in animals injected with *sh-Control* cells in the presence of E2 pellet (Fig. 7b). While none of the animals injected with *sh-Control* cells developed lung metastasis, consistent with our previous study with TMCF7 cells [16], animals that received *sh-UNC5A* cells showed lung metastasis (Fig. 7c). We next examined whether *sh-Control* cell- and *sh-UNC5A* cell-derived tumors differ in angiogenesis because of the differences in *NTN4* expression between *sh-Control* and *sh-UNC5A* cells noted in Fig. 5. *sh-UNC5A* cell-derived tumors contained higher numbers of PECAM1⁺ cells compared with *sh-Control* cell-derived tumors (Fig. 7d), suggesting enhanced angiogenesis in the absence of *UNC5A*.

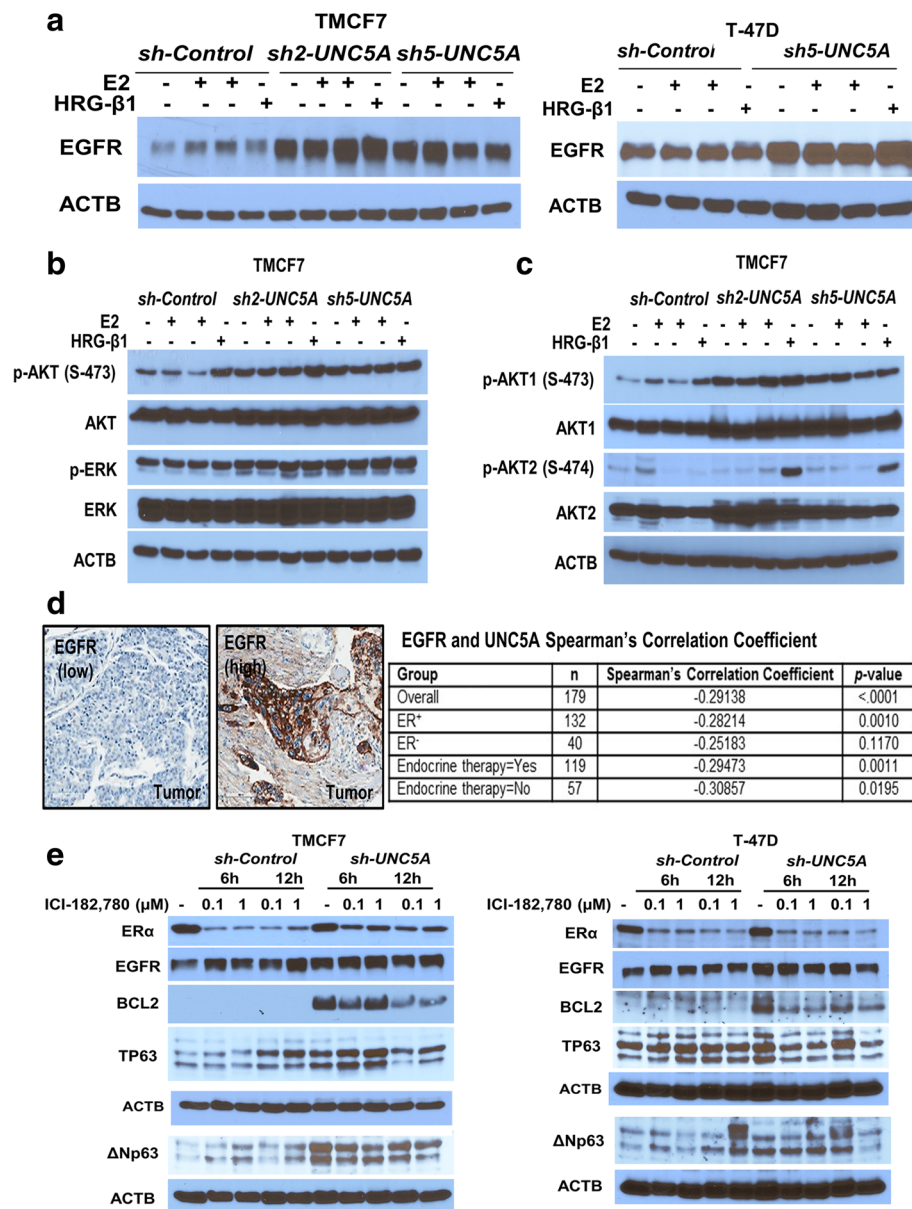


Fig. 6 *UNC5A* knockdown results in elevated epidermal growth factor receptor (EGFR) and phospho-AKT. **a** EGFR protein levels in *sh-Control* and *sh-UNC5A* TMCF7 and T-47D cells. **b** Phospho-AKT and phospho-ERK levels in *sh-Control* and *sh-UNC5A* TMCF7 cells with or without estradiol (E2) or HRG-β1 (20 ng/ml) treatment. Cells were treated with vehicle, E2 for 5 and 15 min, and HRG-β1 for 15 min. **c** Phospho-AKT1 and phospho-AKT2 levels in *sh-Control* and *sh-UNC5A* TMCF7 cells. **d** Representative EGFR staining pattern in breast tumors with low or high expression (left, scale bar = 100 μm). Summary of the correlation analysis between EGFR and UNC5A from breast cancer TMA using Spearman's correlation coefficient (right). UNC5A and EGFR expression was inversely correlated ($p < 0.001$, $n = 179$). **e** Protein levels of estrogen receptor (ER)α, EGFR, BCL2, and TP63 in *sh-Control* and *sh-UNC5A* TMCF7 (left) and T-47D (right) cells after treatment with ICI-182,780 (Fulvestrant)

To determine whether *UNC5A* knockdown enhanced the multiorgan homing capacity of tumor cells, *sh-Control* and *sh-UNC5A* cells were injected via the intracardiac route into animals supplemented with E2 pellets. Autopsies within 17 weeks of injection revealed growth of tumor cells in ovaries and adrenal glands at a higher frequency in animals injected with *sh-UNC5A* cells compared with *sh-Control* cells (Fig. 7e). Histological analysis revealed a

severe disruption of the normal architecture of both organs (Fig. 7f). Ovaries were devoid of follicles and corpora lutea, and the very few remaining were undergoing atresia and degeneration. Likewise, adrenals lost a clear differentiation between the cortex and medulla zones with hemorrhagic areas and high vacuolization even in areas where the capsule is still preserved. Splens of animals that received *sh-UNC5A* cells showed extramedullary

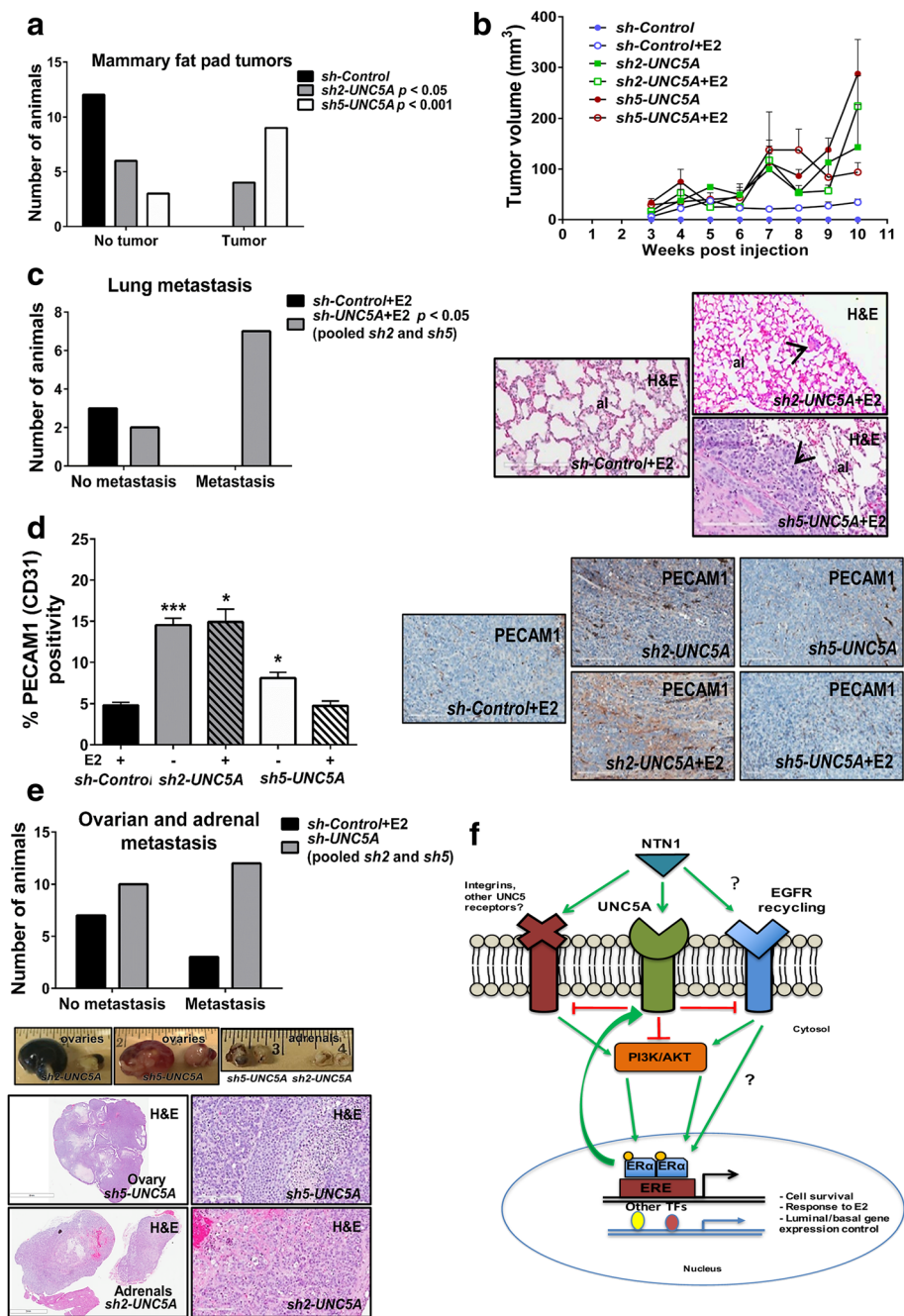


Fig. 7 (See legend on next page.)

(See figure on previous page.)

Fig. 7 *UNC5A* knockdown cells form tumors independent of E2 supplementation. **a** The number of animals with tumors after injection of *sh-Control*, *sh2-UNC5A* and *sh5-UNC5A* TMCF7 cells in the absence of implanted estradiol (E2) pellet. Number of *sh2-UNC5A* ($p < 0.05$) and *sh5-UNC5A* ($p < 0.001$) mammary fat pad tumor-positive mice at the time of euthanasia (11 weeks postinjection). **b** Tumor volume in animals injected with *sh-Control*, *sh2-UNC5A*, or *sh5-UNC5A* TMCF7 cells with or without E2 pellets (mean \pm SEM). **c** Lung metastasis pattern in animals injected with *sh-Control* or *sh-UNC5A* cells into the mammary fat pad in the presence of implanted E2 pellets. The number of animals with and without lung metastasis is shown on the left ($p < 0.05$), whereas representative lung sections stained with hematoxylin and eosin (H&E) from *sh-Control*, *sh2-*, and *sh5-UNC5A* TMCF7 cell inoculated mice with an E2 pellet is shown on the right. Arrowheads point to metastatic tumor cells (al, alveolus; scale bar = 200 μ m). Data were analyzed using the Fisher's exact test (two-tailed). Lungs from only three *sh-Control* cell injected animals were examined because we had previously shown a lack of lung metastasis in animals injected with TMCF7 cells [16]. **d** *sh-UNC5A* TMCF7 cell-derived tumors show significant levels of angiogenesis. PECAM1 staining was performed to measure endothelial cells in tumors. The number of PECAM1⁺ cells in at least 12 fields per tumor is shown on the left, whereas representative PECAM1 staining pattern is shown on the right (scale bar = 200 μ m; * $p < 0.05$ and *** $p < 0.001$). **e** *UNC5A* knockdown cells show enhanced metastases to ovaries and adrenal glands. The number of animals with metastases to ovaries and adrenal glands is shown on the left, whereas the gross appearance of ovaries and adrenal glands of *sh-UNC5A* TMCF7 cells injected via the intracardiac route and the H&E staining pattern of ovary and adrenal gland with metastasis are shown on the right. Scale bars = 3 mm and 200 μ m. **f** Model depicting crosstalk between *UNC5A*, epidermal growth factor receptor (EGFR), and E2 signaling. Unliganded *UNC5A* likely inhibits E2 signaling, which may be reversed upon binding of NTN1. Question marks indicate unknown mechanisms of regulation. ER, estrogen receptor

hematopoiesis with enhanced myeloid and erythroid elements and megakaryocytes causing distention of the spleen in the red pulp area (data not shown). Overall, the results presented above clearly indicate the role of *UNC5A* in regulating the metastasis of ER⁺ tumors and its loss of expression leading to E2-independent growth both in vitro and in vivo.

Discussion

UNC5A is a transmembrane receptor that generates cell survival or death signals in a ligand-dependent manner [10]. *UNC5A* and NTN1 are described as tumor suppressor and oncogene, respectively, in breast cancer [51, 52]. However, signaling pathways that control their expression to alter the balance between *UNC5A* and NTN1 are unknown. Analyses of TCGA dataset showed elevated expression of *UNC5A* in luminal breast cancers, and NTN1 overexpression in TNBCs and E2 could further enhance luminal expression of *UNC5A* (Fig. 1). Thus, the *UNC5A*–NTN1 signaling axis is likely tilted more towards *UNC5A*-activated signals in ER⁺/PR⁺ breast cancers and NTN1-generated signals in TNBC/ER⁻ tumors. Consistent with this possibility, *UNC5A* expression was prognostic in ER⁺/PR⁺/HER2⁻ breast cancers but not in ER⁻ tumors, suggesting its critical role in ER⁺/PR⁺/HER2⁻ breast cancers. A subgroup of women with ER⁺/PR⁺ breast cancers develop recurrence, and molecular assays such as the Recurrence Score and Breast Cancer Index are helping to identify ER⁺/PR⁺ breast cancer patients requiring hormonal and/or chemotherapy [53]. *UNC5A*, possibly in combination with EGFR, could be developed as a biomarker to identify such patients [4].

Molecular events causing variable *UNC5A* expression in ER⁺ tumors are unknown. *UNC5A* is a TP53-inducible gene, and TP53 is infrequently mutated in ER⁺/PR⁺ breast cancer [2, 54]. Deregulated p53 activity instead of mutations may lead to loss of *UNC5A*

expression in ER⁺/PR⁺ tumors, although this remains to be investigated. In addition, there is potential for p53 to control *UNC5A* activity since we noted a differential effect of *UNC5A* knockdown on proliferation in wild-type p53 containing MCF7 cells compared with mutant p53 containing T-47D cells, although knockdown had a similar effect on BCL2 and TP63 expression in both cell lines. cBioPortal analyses revealed frequent missense and truncating mutations in *UNC5A* [55]. Additionally, *UNC5A* expression is regulated through allele-specific DNA methylation [56]. Thus, mutations and DNA methylation could be other mechanisms leading to inactivation/silencing of *UNC5A* during breast cancer progression.

One of the consequences of reduced *UNC5A* expression is significant changes in basal gene expression and altered ER α signaling. GO analyses revealed a specific effect of *UNC5A* knockdown on a network of transcription factors including the stem cell-associated transcription factor *SOX2*, which may be a reason for the altered expression of 20% of genes in *sh-UNC5A* MCF7 cells and 7% in *sh-UNC5A* T-47D cells compared with *sh-Control* cells (Fig. 4). It is interesting that, in both cell lines, *UNC5A* knockdown affected the expression of genes linked to the plasma membrane and extracellular region composition (Fig. 4), which can explain the aggressive growth characteristics of *sh-UNC5A* compared with *sh-Control* MCF7 cells in vivo. We also observed a distinct effect of *UNC5A* on E2-regulated gene expression, with several genes gaining E2-regulated gene expression (Fig. 4). These results suggest a role for *UNC5A* in restricting the activity of unliganded ER α in a gene-specific manner, which could involve the following mechanisms. One possibility is the direct effect of *UNC5A*-activated signals on chromatin organization since we observed an effect of *UNC5A* knockdown on the histone demethylation network in E2-treated cells (Fig. 4). *UNC5A* knockdown increased the E2-inducible expression of KDM4B, which is a master regulator of

ER α activity [57]. Elevated KDM4B in *sh-UNC5A* cells could further amplify the E2 signaling axis as evident from more than 400 genes gaining E2-regulated expression in *sh-UNC5A* cells. Robustness at which *UNC5A* knockdown altered BCL2 expression further suggests a direct link between *UNC5A* and chromatin organization. This drastic effect of *UNC5A* knockdown on BCL2 expression is reminiscent of permanent gene expression changes observed upon transient knockdown of DNMT1 [38]. However, we did not observe an effect of *UNC5A* knockdown on the expression of any DNMTs, although there was a modest but statistically significant effect on *TET1* and *TET3* which antagonize DNMTs (Additional file 6). *UNC5A* knockdown may have an effect on histone acetylation/deacetylation since *sh-UNC5A* MCF7 cells expressed significantly higher levels of the epigenetic regulator *HDAC9* compared with *sh-Control* cells (Additional files 6). The second possibility is the involvement of *ELF5*. *ELF5* suppresses E2 sensitivity by reducing the expression of *ESR1* and the pioneer factors *FOXA1* and *GATA3* [36]. ER α , *FOXA1*, and *GATA3* constitute a positive lineage-restricted hormone responsive regulatory loop in luminal cells [58]. We observed the effect of *UNC5A* knockdown on *ELF5* expression, and reduced *ELF5* expression in *sh-UNC5A* MCF7 cells correlated with elevated *GATA3* expression (Additional file 6). The third possibility is the involvement of *AKT*. *UNC5A* knockdown caused upregulation of activated *AKT*, which confers ligand-independent activity to ER α [59]. The fourth possibility involves ER α -EGFR cross-talk since *UNC5A* knockdown cells contained higher levels of EGFR protein (Fig. 7), and EGF through EGFR has been shown to alter ER α cistrome and transcriptome [60].

UNC5A knockdown in MCF7 cells resulted in a hybrid phenotype with cells expressing luminal (ER, *PGR*), myoepithelial (TP63), and stem cell markers (*SOX2*), which in part is due to altered ER α signaling. Recent studies have identified similar hybrid cells in primary breast cancers, potentially generated through Notch-Jagged signaling [42, 61]. Based on cell surface marker profiles and KRT14/KRT19 expression patterns in *sh-UNC5A* cells, we propose that the gradual loss of *UNC5A* results in cancer cells acquiring hybrid phenotype without expressing classic markers of EMT. Since there is still a controversy related to in-vivo detection of cancer cells with EMT features, it is possible that primary tumors contain cells with hybrid phenotype which functionally behave like cancer cells with EMT features. Characterizing primary tumors for ER, PR, *UNC5A*, EGFR, and additional basal cell markers would allow the detection of such hybrid cells. Collectively, results presented in this study provide novel insights into pathways that restrict ER α signaling and metastatic progression of

ER α ⁺ breast cancer, which potentially involves luminal to luminal/basal hybrid conversion due to an aberrant DR pathway.

Conclusions

In this study, we demonstrate an unexpected role for the dependence receptor *UNC5A* in regulating ER α activity and restricting the expression of basal cell-enriched genes in luminal cells. Progressive loss of *UNC5A* expression could result in ER α -positive luminal cells acquiring basal features including the expression of Δ Np63, *SOX2*, and EGFR, while maintaining ER α expression. These results describe the role of *UNC5A* in controlling plasticity of luminal breast cancer. Therefore, *UNC5A*, ER α , and EGFR could be developed as markers to identify luminal breast cancers with a potential for subtype conversion.

Additional files

Additional file 1: Tables that describe antibodies and primers used in the study. (DOCX 121 kb)

Additional file 2: E2-regulated expression of *UNC5A* in various cell types extracted from published studies using NURSA data resource. (XLSX 13 kb)

Additional file 3: Description of patients and characteristics of their tumors ($n = 221$). (DOCX 98 kb)

Additional file 4: Summary of results of overall survival: univariate and multivariate analyses on the *UNC5A H* score category. (DOCX 96 kb)

Additional file 5: The effect of ICI-182,780 (Fulvestrant) treatment on *UNC5A* knockdown cells and Western blot showing *UNC5A* knockdown by CRISPR in MCF-7 cells. (PSD 3346 kb)

Additional file 6: Summary of results of RNA-seq of *sh-Control* and *sh5-UNC5A* clones of MCF7 and T-47D cells. Various comparisons are shown. (XLSX 859 kb)

Additional file 7: Pathways analyses using DAVID of differentially expressed genes under different conditions and in different cell types. (XLSX 139 kb)

Additional file 8: Characterization of TMCF7 cells with and without *UNC5A* knockdown for stemness and luminal/basal hybrid features. (PSD 50580 kb)

Abbreviations

ACTB: Beta-actin; AKT: v-AKT murine thymoma viral oncogene; APOBEC3B: Apolipoprotein B mRNA-editing enzyme; BCL2: B cell leukemia/lymphoma 2; CCS: Charcoal-dextran treated fetal calf serum; ChIP: Chromatin immunoprecipitation; CSC: Cancer stem cell; DEG: Differentially expressed gene; DNMT1: DNA methyltransferase 1; DR: Dependence receptor; E2: Estradiol; EGFR: Epidermal growth factor receptor; ELISA: Enzyme-linked immunosorbent assay; EMT: Epithelial to mesenchymal transition; ER: Estrogen receptor; ERE: Estrogen response element; ERK: Extracellular signal-regulated kinase; FC: Fold change; FDR: False discovery rate; GEO: Gene expression omnibus; GO: Gene ontology; H&E: Hematoxylin and eosin; HRG: Heregulin; MEM: Minimum essential media; NTN: Netrin; OHT: 4-Hydroxy tamoxifen; PBS: Phosphate-buffered saline; PR: Progesterone receptor; qRT-PCR: Quantitative reverse transcription polymerase chain reaction; shRNA: Short hairpin RNA; TCGA: The Cancer Genome Atlas; TMA: Tissue microarray; TNBC: Triple negative breast cancer; *UNC5A*: Unc-5 netrin receptor A

Acknowledgments

We thank Dr. Hitesh Appaiah for initial analysis of UNC5A expression in breast cancer cell lines, the IU Simon Cancer Center Flow Cytometry Core for flow cytometry, and the Tissue Procurement facility of IUSCC for the TMA.

Funding

Susan G. Komen for the Cure SAC110025 provided financial support for this work (HN). The Vera Bradley Foundation for Breast Cancer Scholar Program at the IU Simon Cancer Center provided support to MBP. Collaborative Care for Cancer Bioinformatics, supported by the Walther Cancer Foundation, performed the bioinformatics analyses of RNA-seq data.

Availability of data and materials

RNA-seq data has been deposited with GEO under the accession number GSE89700. All cell lines will be made available upon request.

Authors' contributions

MBP: in-vitro experiments, maintained animal colonies, tumor measurements and harvesting, analyzed data, and wrote the manuscript; PBN: in-vitro experiments including ChIP assays, cell proliferation assays, and Western blotting; MA: cancer stem cell-related work including flow cytometry and mammospheres; MSP: immunofluorescence; YH: RNA-seq data analyses; XR: ChIP-seq and expression data alignment; SL: Bioinformatics analyses of RNA-seq data; JW: Bioinformatics analyses of RNA-seq data; YL: RNA-seq analyses; KM: histopathology; MJ: EGFR immunohistochemistry scoring; GS: pathologist who evaluated TMA and tissues from xenograft studies; SA: statistical analyses of TMA; SP: statistical analyses of TMA; HN: overall study design, mammary fat pad and intracardiac injection, data interpretation, and manuscript writing. All authors have read and approved the final manuscript.

Ethics approval and consent to participate

Tumor samples used in the tissue microarray were obtained after informed consent and the Indiana University Institutional Review Board has approved the use of human tissue. Participants have consented for publication. The article does not contain data from individual participants. All animal studies were performed as per NIH guidelines and with approval from the Institutional Animal Care and Use Committee.

Competing interests

The authors declare that they have no competing interests.

Publisher's Note

Springer Nature remains neutral with regard to jurisdictional claims in published maps and institutional affiliations.

Author details

¹Department of Surgery, Indiana University School of Medicine, Indianapolis, IN 46202, USA. ²Department of Medical and Molecular Genetics, Indiana University School of Medicine, Indianapolis, IN 46202, USA. ³Center for Computational Biology and Bioinformatics, Indiana University School of Medicine, Indianapolis, IN 46202, USA. ⁴Department of Pathology and Laboratory Medicine, Indiana University School of Medicine, Indianapolis, IN 46202, USA. ⁵Department of Biostatistics, Indiana University School of Medicine, Indianapolis, IN 46202, USA. ⁶Department of Biochemistry and Molecular Biology, Indiana University School of Medicine, Indianapolis, IN 46202, USA. ⁷VA Roudebush Medical Center, C218C, 980 West Walnut St, Indianapolis, IN 46202, USA. ⁸Present Address: Department of Pediatrics and Herman B. Wells Center for Pediatrics Research, Indiana University School of Medicine, Indianapolis, IN, USA.

Received: 10 October 2017 Accepted: 23 March 2018

Published online: 02 May 2018

References

- Ali S, Coombes RC. Endocrine-responsive breast cancer and strategies for combating resistance. *Nat Rev Cancer*. 2002;2(2):101–12.
- Sorlie T, Perou CM, Tibshirani R, Aas T, Geisler S, Johnsen H, Hastie T, Eisen MB, van de Rijn M, Jeffrey SS, et al. Gene expression patterns of breast carcinomas distinguish tumor subclasses with clinical implications. *Proc Natl Acad Sci U S A*. 2001;98(19):10869–74.
- Ades F, Zardavas D, Bozovic-Spasojevic I, Pugliano L, Fumagalli D, de Azambuja E, Viale G, Sotiriou C, Piccart M. Luminal B breast cancer: molecular characterization, clinical management, and future perspectives. *J Clin Oncol*. 2014;32(25):2794–803.
- Cejalvo JM, Martinez de Duenas E, Galvan P, Garcia-Recio S, Burgues Gasion O, Pare L, Antolin S, Martinello R, Blancas I, Adamo B, et al. Intrinsic subtypes and gene expression profiles in primary and metastatic breast cancer. *Cancer Res*. 2017;77:2213–21.
- Ellis MJ, Tao Y, Young O, White S, Proia AD, Murray J, Renshaw L, Faratian D, Thomas J, Dowsett M, et al. Estrogen-independent proliferation is present in estrogen-receptor HER2-positive primary breast cancer after neoadjuvant letrozole. *J Clin Oncol*. 2006;24(19):3019–25.
- Zaret KS, Carroll JS. Pioneer transcription factors: establishing competence for gene expression. *Genes Dev*. 2011;25(21):2227–41.
- Badve S, Turbin D, Thorat MA, Morimiya A, Nielsen TO, Perou CM, Dunn S, Huntsman DG, Nakshatri H. FOXA1 expression in breast cancer correlation with luminal subtype A and survival. *Clin Cancer Res*. 2007;13(15):4415–21.
- Ma CX, Reinert T, Chmielewska I, Ellis MJ. Mechanisms of aromatase inhibitor resistance. *Nat Rev Cancer*. 2015;15(5):261–75.
- Bhat-Nakshatri P, Wang G, Appaiah H, Luktuke N, Carroll JS, Geistlinger TR, Brown M, Badve S, Liu Y, Nakshatri H. AKT alters genome-wide estrogen receptor alpha binding and impacts estrogen signaling in breast cancer. *Mol Cell Biol*. 2008;28(24):7487–503.
- Mehlen P, Bredesen DE. Dependence receptors: from basic research to drug development. *Sci Signal*. 2011;4(157):mr2.
- Arakawa H. Netrin-1 and its receptors in tumorigenesis. *Nat Rev Cancer*. 2004;4(12):978–87.
- Cirulli V, Yebra M. Netrins: beyond the brain. *Nat Rev Mol Cell Biol*. 2007;8(4):296–306.
- Mehlen P, Delloye-Bourgeois C, Chedotal A. Novel roles for Slits and netrins: axon guidance cues as anticancer targets? *Nat Rev Cancer*. 2011;11(3):188–97.
- Perkins SM, Bales C, Vladislav T, Althouse S, Miller KD, Sandusky G, Badve S, Nakshatri H. TFAP2C expression in breast cancer: correlation with overall survival beyond 10 years of initial diagnosis. *Breast Cancer Res Treat*. 2015; 152(3):519–31.
- McCune K, Bhat-Nakshatri P, Thorat M, Nephew KP, Badve S, Nakshatri H. Prognosis of hormone-dependent breast cancers: implications of the presence of dysfunctional transcriptional networks activated by insulin via the immune transcription factor T-bet. *Cancer Res*. 2010;70:685–96. PMID:20068169.
- Kumar S, Kishimoto H, Chua HL, Badve S, Miller KD, Bigsby RM, Nakshatri H. Interleukin-1 alpha promotes tumor growth and cachexia in MCF-7 xenograft model of breast cancer. *Am J Pathol*. 2003;163(6):2531–41.
- Bhat-Nakshatri P, Goswami CP, Badve S, Magnani L, Lupien M, Nakshatri H. Molecular insights of pathways resulting from two common PIK3CA mutations in breast cancer. *Cancer Res*. 2016;76(13):3989–4001.
- Miller DF, Yan PS, Buechlein A, Rodriguez BA, Yilmaz AS, Goel S, Lin H, Collins-Burow B, Rhodes LV, Braun C, et al. A new method for stranded whole transcriptome RNA-seq. *Methods*. 2013;63(2):126–34.
- Dobin A, Davis CA, Schlesinger F, Drenkow J, Zaleski C, Jha S, Batut P, Chaisson M, Gingeras TR. STAR: ultrafast universal RNA-seq aligner. *Bioinformatics*. 2013;29(1):15–21.
- Liao Y, Smyth GK, Shi W. featureCounts: an efficient general purpose program for assigning sequence reads to genomic features. *Bioinformatics*. 2014;30(7):923–30.
- Robinson MD, McCarthy DJ, Smyth GK. edgeR: a bioconductor package for differential expression analysis of digital gene expression data. *Bioinformatics*. 2010;26(1):139–40.
- McCarthy DJ, Chen Y, Smyth GK. Differential expression analysis of multifactor RNA-Seq experiments with respect to biological variation. *Nucleic Acids Res*. 2012;40(10):4288–97.
- Huang DW, Sherman BT, Tan Q, Collins JR, Alvord WG, Roayaei J, Stephens R, Baseler MW, Lane HC, Lempicki RA. The DAVID gene functional classification tool: a novel biological module-centric algorithm to functionally analyze large gene lists. *Genome Biol*. 2007;8(9):R183.
- Huang da W, Sherman BT, Lempicki RA. Systematic and integrative analysis of large gene lists using DAVID bioinformatics resources. *Nat Protoc*. 2009;4(1):44–57.
- Bhat-Nakshatri P, Goswami CP, Badve S, Sledge GW Jr, Nakshatri H. Identification of FDA-approved drugs targeting breast cancer stem cells along with biomarkers of sensitivity. *Sci Rep*. 2013;3:2530.

26. Nakshatri H, Anjanappa M, Bhat-Nakshatri P. Ethnicity-dependent and -independent heterogeneity in healthy normal breast hierarchy impacts tumor characterization. *Sci Rep*. 2015;5:13526.
27. Welboren WJ, van Driel MA, Janssen-Megens EM, van Heeringen SJ, Sweep FC, Span PN, Stunnenberg HG. ChIP-Seq of ERalpha and RNA polymerase II defines genes differentially responding to ligands. *EMBO J*. 2009;28(10):1418–28.
28. Chandrashekar DS, Bachelot T, Bachelot A, Balasubramanya SAH, Creighton CJ, Ponce-Rodriguez I, Chakravarthi B, Varambally S. UALCAN: a portal for facilitating tumor subgroup gene expression and survival analyses. *Neoplasia*. 2017;19(8):649–58.
29. Dressing GE, Knutson TP, Schiewer MJ, Daniel AR, Hagan CR, Diep CH, Knudsen KE, Lange CA. Progesterone receptor-cyclin D1 complexes induce cell cycle-dependent transcriptional programs in breast cancer cells. *Mol Endocrinol*. 2014;28(4):442–57.
30. Svtelisl A, Bianco S, Madore J, Huppe G, Nordell-Markovits A, Mes-Masson AM, Gevry N. H3K27 demethylation by JMJD3 at a poised enhancer of anti-apoptotic gene BCL2 determines ERalpha ligand dependency. *EMBO J*. 2011;30(19):3947–61.
31. Cannuyer J, Van Tongelen A, Lorient A, De Smet C. A gene expression signature identifying transient DNMT1 depletion as a causal factor of cancer-germline gene activation in melanoma. *Clin Epigenetics*. 2015;7:114.
32. Periyasamy M, Patel H, Lai CF, Nguyen VT, Nevedomskaya E, Harrod A, Russell R, Remenyi J, Ochocka AM, Thomas RS, et al. APOBEC3B-mediated cytidine deamination is required for estrogen receptor action in breast cancer. *Cell Rep*. 2015;13(1):108–21.
33. Hyun K, Jeon J, Park K, Kim J. Writing, erasing and reading histone lysine methylations. *Exp Mol Med*. 2017;49(4):e324.
34. Vizan P, Beringer M, Ballare C, Di Croce L. Role of PRC2-associated factors in stem cells and disease. *FEBS J*. 2015;282(9):1723–35.
35. Melino G, Memmi EM, Pelicci PG, Bernassola F. Maintaining epithelial stemness with p63. *Sci Signal*. 2015;8(387):re9.
36. Kalyuga M, Gallego-Ortega D, Lee HJ, Roden DL, Cowley MJ, Caldon CE, Stone A, Allerdice SL, Valdes-Mora F, Launchbury R, et al. ELF5 suppresses estrogen sensitivity and underpins the acquisition of antiestrogen resistance in luminal breast cancer. *PLoS Biol*. 2012;10(12):e1001461.
37. Singh S, Pradhan AK, Chakraborty S. SUMO1 negatively regulates the transcriptional activity of EVI1 and significantly increases its co-localization with EVI1 after treatment with arsenic trioxide. *Biochim Biophys Acta*. 2013;1833(10):2357–68.
38. Larriue-Lahargue F, Welm AL, Thomas KR, Li DY. Netrin-4 induces lymphangiogenesis in vivo. *Blood*. 2010;115(26):5418–26.
39. Malzahn K, Mitze M, Thoenes M, Moll R. Biological and prognostic significance of stratified epithelial cytokeatins in infiltrating ductal breast carcinomas. *Virchows Arch*. 1998;433(2):119–29.
40. Villadsen R, Fridriksdottir AJ, Ronnov-Jessen L, Gudjonsson T, Rank F, LaBarge MA, Bissell MJ, Petersen OW. Evidence for a stem cell hierarchy in the adult human breast. *J Cell Biol*. 2007;177(1):87–101.
41. Bates RC, Bellovin DI, Brown C, Maynard E, Wu B, Kawakatsu H, Sheppard D, Oettgen P, Mercurio AM. Transcriptional activation of integrin beta6 during the epithelial-mesenchymal transition defines a novel prognostic indicator of aggressive colon carcinoma. *J Clin Invest*. 2005;115(2):339–47.
42. Grosse-Wilde A, Fouquier d'Herouel A, McIntosh E, Ertaylan G, Skupin A, Kuestner RE, del Sol A, Walters KA, Huang S. Stemness of the hybrid epithelial/mesenchymal state in breast cancer and its association with poor survival. *PLoS One*. 2015;10(5):e0126522.
43. Visvader JE, Stingl J. Mammary stem cells and the differentiation hierarchy: current status and perspectives. *Genes Dev*. 2014;28(11):1143–58.
44. Al-Hajj M, Wicha MS, Benito-Hernandez A, Morrison SJ, Clarke MF. Prospective identification of tumorigenic breast cancer cells. *Proc Natl Acad Sci U S A*. 2003;100(7):3983–8.
45. Sarkar A, Hochedlinger K. The sox family of transcription factors: versatile regulators of stem and progenitor cell fate. *Cell Stem Cell*. 2013;12(1):15–30.
46. Osborne CK, Schiff R. Mechanisms of endocrine resistance in breast cancer. *Annu Rev Med*. 2011;62:233–47.
47. Lupien M, Meyer CA, Bailey ST, Eeckhoutte J, Cook J, Westerling T, Zhang X, Carroll JS, Rhodes DR, Liu XS, et al. Growth factor stimulation induces a distinct ER(alpha) cistrome underlying breast cancer endocrine resistance. *Genes Dev*. 2010;24(19):2219–27.
48. Valentin MD, da Silva SD, Privat M, Alaoui-Jamali M, Bignon YJ. Molecular insights on basal-like breast cancer. *Breast Cancer Res Treat*. 2012;134(1):21–30.
49. Plissonnier ML, Lahlali T, Michelet M, Lebosse F, Cottarel J, Beer M, Neveu G, Durantel D, Bartosch B, Accardi R, et al. Epidermal growth factor receptor-dependent mutual amplification between Netrin-1 and the hepatitis C virus. *PLoS Biol*. 2016;14(3):e1002421.
50. Sweeney CJ, Mehrotra S, Sadaria MR, Kumar S, Shortle NH, Roman Y, Sheridan C, Campbell RA, Murry DJ, Badve S, et al. The sesquiterpene lactone parthenolide in combination with docetaxel reduces metastasis and improves survival in a xenograft model of breast cancer. *Mol Cancer Ther*. 2005;4(6):1004–12.
51. Fitamant J, Guenebeaud C, Coissieux MM, Guix C, Treilleux I, Scoazec JY, Bachelot T, Bernet A, Mehlen P. Netrin-1 expression confers a selective advantage for tumor cell survival in metastatic breast cancer. *Proc Natl Acad Sci U S A*. 2008;105(12):4850–5.
52. Thiebault K, Mazelin L, Pays L, Llambi F, Joly MO, Scoazec JY, Saurin JC, Romeo G, Mehlen P. The netrin-1 receptors UNC5H are putative tumor suppressors controlling cell death commitment. *Proc Natl Acad Sci U S A*. 2003;100(7):4173–8.
53. Sestak I, Zhang Y, Schroeder BE, Schnabel CA, Dowsett M, Cuzick J, Sgroi D. Cross-stratification and differential risk by breast cancer index and recurrence score in women with hormone receptor-positive lymph node-negative early-stage breast cancer. *Clin Cancer Res*. 2016;22(20):5043–8.
54. Miyamoto Y, Futamura M, Kitamura N, Nakamura Y, Baba H, Arakawa H. Identification of UNC5A as a novel transcriptional target of tumor suppressor p53 and a regulator of apoptosis. *Int J Oncol*. 2010;36(5):1253–60.
55. Cerami E, Gao J, Dogrusoz U, Gross BE, Sumer SO, Aksoy BA, Jacobsen A, Byrne CJ, Heuer ML, Larsson E, et al. The cBio cancer genomics portal: an open platform for exploring multidimensional cancer genomics data. *Cancer discovery*. 2012;2(5):401–4.
56. Wang J, Valo Z, Bowers CW, Smith DD, Liu Z, Singer-Sam J. Dual DNA methylation patterns in the CNS reveal developmentally poised chromatin and monoallelic expression of critical genes. *PLoS One*. 2010;5(11):e13843.
57. Gaughan L, Stockley J, Coffey K, O'Neill D, Jones DL, Wade M, Wright J, Moore M, Tse S, Rogerson L, et al. KDM4B is a master regulator of the estrogen receptor signalling cascade. *Nucleic Acids Res*. 2013;41(14):6892–904.
58. Eeckhoutte J, Keeton EK, Lupien M, Krum SA, Carroll JS, Brown M. Positive cross-regulatory loop ties GATA-3 to estrogen receptor alpha expression in breast cancer. *Cancer Res*. 2007;67(13):6477–83.
59. Campbell RA, Bhat-Nakshatri P, Patel NM, Constantinidou D, Ali S, Nakshatri H. Phosphatidylinositol 3-kinase/AKT-mediated activation of estrogen receptor alpha: a new model for anti-estrogen resistance. *J Biol Chem*. 2001;276(13):9817–24.
60. Lupien MMC, Bailey ST, Eeckhoutte J, Cook J, Westerling T, Zhang X, Carroll JS, Rhodes DR, Liu XS, Brown M. Growth factor stimulation induces a distinct ERalpha cistrome underlying breast cancer endocrine resistance. *Genes Dev*. 2010;24:2219–27.
61. Boareto M, Jolly MK, Goldman A, Pietila M, Mani SA, Sengupta S, Ben-Jacob E, Levine H, Onuchic JN. Notch-Jagged signalling can give rise to clusters of cells exhibiting a hybrid epithelial/mesenchymal phenotype. *J R Soc Interface*. 2016;13(118). doi: <https://doi.org/10.1098/rsif.2015.1106>.

Submit your next manuscript to BioMed Central and we will help you at every step:

- We accept pre-submission inquiries
- Our selector tool helps you to find the most relevant journal
- We provide round the clock customer support
- Convenient online submission
- Thorough peer review
- Inclusion in PubMed and all major indexing services
- Maximum visibility for your research

Submit your manuscript at
www.biomedcentral.com/submit

